Summary of Thesis

Modification of Metal Oxide Doped Polymer Nanocomposites using Ion Beam Irradiation

A THESIS, SUBMITTED BY

SHILPABEN NARENDRABHAI BHAVSAR

FOR THE AWARD OF THE DEGREE OF

DOCTOR OF PHILOSOPHY

IN

PHYSICS

UNDER THE GUIDANCE OF

Prof. N. L. Singh

PHYSICS DEPARTMENT
FACULTY OF SCIENCE
THE MAHARAJA SAYAJIRAO UNIVERSITY OF BARODA
VADODARA-390002, GUJARAT, INDIA

MAY-2021

The polymer has shown its potential application in all fields, particularly in the fields of medical science, electronics and optical devices [1–3]. Nevertheless, the performances of polymers are sometimes shown to be inadequate, especially as regards their mechanical and thermal properties [4,5]. There are various ways to get content that meets the required criteria. Many techniques are available to improve the properties of polymers, such as the incorporation of nanoparticles or salts, irradiation techniques and many more [6]. The incorporation of nanofiller in polymers makes them novel materials/nanocomposites, which are proposed to potential in the field of battery, gas sensors, photo-electronic devices, catalysis, electrochemistry and optical devices [3,7,8].

Research in the use of noble nanomaterials has mushroomed over the last few decades, and significantly, numerous works have been executed to understand the nanomaterials and their composites. By confinement of materials in nanometre spatial dimensions, small size effect, surface effect, quantum size effect and macroscopic quantum tunnel effect can alter the optical, luminescence, electrical and structural properties [9]. Considerable works have been done to investigate the structural, optical and electrical properties of polymer nanocomposites. The luminescence properties of polymers can be improved dramatically by doping metal oxide, rare earth metal oxides, metal and so on.

The application of ionizing radiation in polymeric materials and polymer nanocomposites has grown since the physical and chemical properties of the polymers can be modified in a controlled way. Important properties of polymer nanocomposites that are mechanical, thermal stability, chemical resistance, melt flow, optical and surface properties significantly improved by irradiation [10]. Interest has also evolved in the peculiar nature of the ion-polymer interaction. It is also important to understand the effect of irradiation on a more fundamental level how the polymer interacts with nanofillers. The field of polymer nanocomposites modification by gamma and ion beam, and its characterization has become a very challenging field owing to vast technological implications [11]. The primary phenomena associated with the interaction of radiation with the polymers are chain scission, chain aggregation, crosslinking, double bonds formation and so on. Various gaseous species are released during irradiation. Radiation degradation is a random chain scission process that reduces the molecular weight of the polymer, thus, plasticizing the material [12,13].

All these effects depend on the composition, density, molecular weight of the polymer, time of irradiation, mass, energy, charge and fluence of the ion beam [14].

The present work aims to investigate gamma-ray and carbon ion irradiations on structural, optical, luminescence, electrical properties and surface morphology of polymer composites. All the samples investigated were prepared using the solution casting method. Al_2O_3, Eu_2O_3 and SiO_2 were selected as nanofillers while Polystyrene and Polyvinyl alcohol were selected as polymer matrices. The pristine and irradiated polymeric films were characterized using powder X-ray diffraction (XRD), Fourier Transform Infrared (FT-IR) Spectroscopy, photoluminescence, thermoluminescence, UV-Visible spectroscopy, impedance spectroscopy, differential scanning calorimetry, and atomic force microscopy.

The whole work is listed in the thesis and divided into the following chapters:

Chapter 1 covers an outline of polymer and polymer composites, followed by their classification and applications. The relevant literature survey is presented and, the aims/objectives of the present work have been stated.

Chapter 2 contains the basic information of the material that is used in the present investigation. It also contains the fundamental details of the characterization techniques used to characterize the synthesized and irradiated nanocomposites.

Chapter 3 deals with the effects of gamma and carbon ion beam irradiation on optical, luminescence, electrical and thermal properties of PS/Al_2O_3 nanocomposites as a function of filler concentration and irradiation dose.

The diffraction patterns of nanocomposites showed a broad peak at 2θ = 19.76°, indicating that the polymeric film is partially crystalline and leading to an amorphous nature. The inclusion of aluminum oxide nanoparticles does not alter the XRD pattern of PS. Also, no other peaks are found in XRD pattern of PS. The EDAX patterns of PS/Al_2O_3 nanocomposites indicate the presence of aluminum oxide in the polymer matrix. In FTIR spectra, the new band at 450 cm^{-1} appeared in the FTIR spectra of nanocomposites are assigned to stretching vibration of Al-O bond. FTIR analysis displays a decrease in the peak intensity after incorporation of nanofiller and SHI irradiation. This suggests randomization of macromolecular chains and degradation at backbones and side-chains of the macromolecular structure by removing hydrogen atoms. FTIR spectra of nanocomposites do not change upon gamma irradiation due to the presence of benzene rings [15]. Optical absorption measurements of the prepared nanocomposites show a redshift in the absorption edge

with nanofiller level and irradiation dose. UV– Vis spectroscopy shows a decrease in optical bandgap with the increase in nanofiller concentration and irradiation dose. The change in optical bandgap due to both types of irradiation is different, the phenomenon is characterized by the density of state model in Non-crystalline material as proposed by Mott and Davis [16].

Figure 3.1 (a) depicts the excitation spectrum of polymer nanocomposites, observed at an emission wavelength of 435 nm. It shows a broad excitation band centered around 380 nm. The emission spectra of nanocomposites comprise three peaks at 411 nm, 435 nm and 462 nm with excitation wavelength at 380 nm, as shown in **Figure 3.1** (b). The intensity of PL emission peaks has been observed to increase with the increase in filler levels and irradiation dose. It indicates that new radiative recombination is associated with dose, resulting in the change in the configuration of the facial layer. Hence the rate of radiation transition escalates with irradiation dose [17,18].

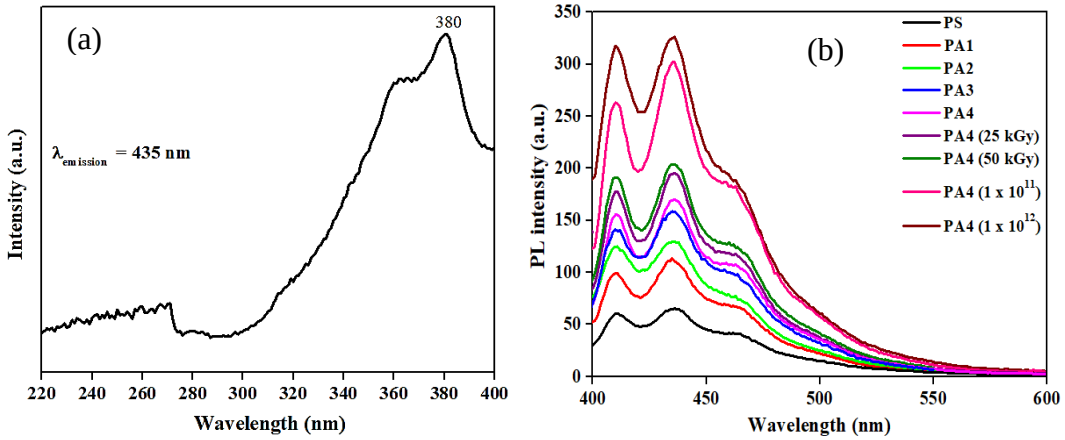

Figure 3.1 (a) PL excitation spectra of PS at the emission wavelength of 435 nm (b) PL emission spectra of pristine and irradiated PS-based polymer nanocomposites at the excitation wavelength of 380 nm.

Figure 3.2. TL glow curves of polymer composites are comprised of several TL maxima. Different molecular relaxations such as δ-,γ- and β - relaxations are related to maximum temperature at maximum intensity (Tm).

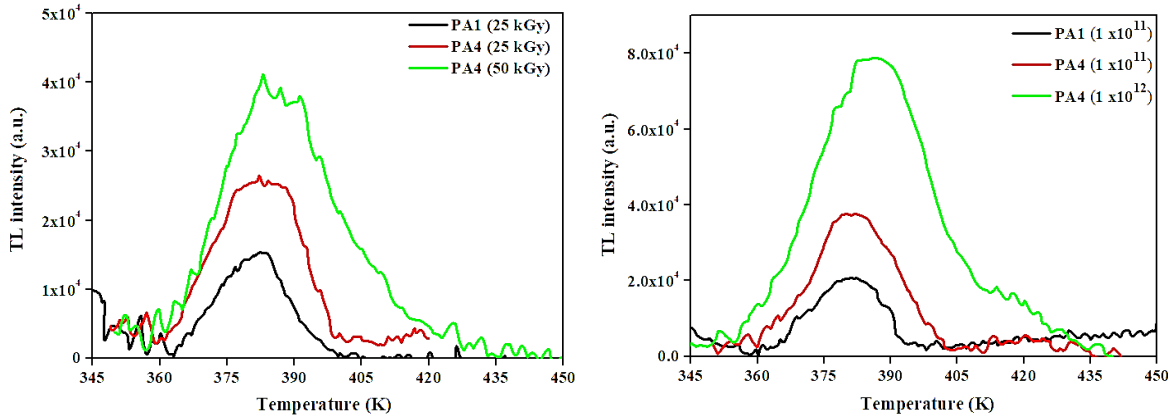

Figure 3.2 TL glow curves of (a) gamma-irradiated polymer composites (b) 90 MeV Carbon ions irradiated polymer composites.

TL glow curve intensity shows an increase with dose, which may indicate an increase in the number of trapping centers upon irradiation. Moreover, the change in the intensity of TL glow curve for SHI irradiated samples is more pervasive than for gamma-irradiated ones. It could be concluded that the energy deposited by gamma rays and C^{6+} ions formed similar types of defects and trapping centers at various depths in polymer nanocomposites [19].

Figure 3.3 depicts the variation of (a) dielectric constants and (b) dielectric loss of pristine and irradiated polymer nanocomposites. As the concentration of filler increases, the overall response of dielectric constants and dielectric loss increases due to the interfacial polarization effect between filler and polymer matrices. Moreover, an increase in the dielectric constant with dose indicates the formation of low molecular polymeric macromolecules in the lower frequency region.

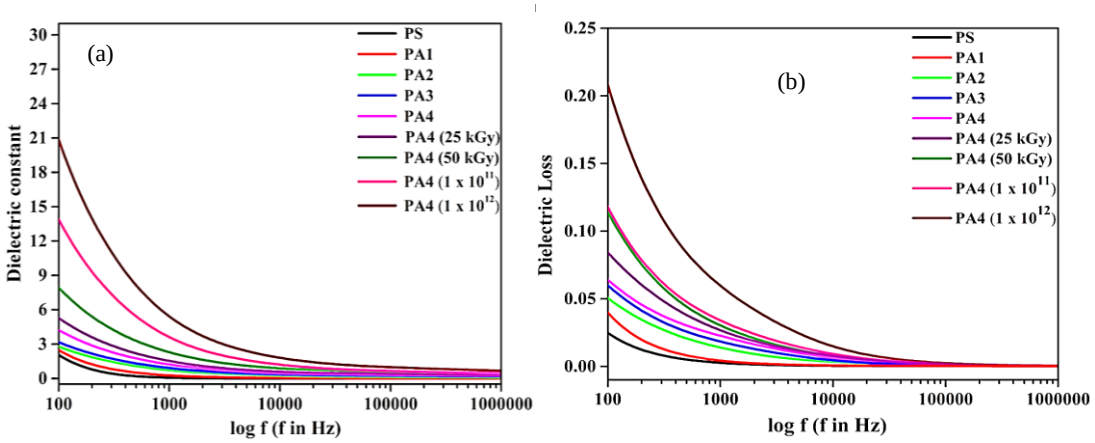

Figure 3.3 Variation in (a) dielectric constant and (b) dielectric loss versus frequency, for polymer nanocomposites with the concentration of filler and dose.

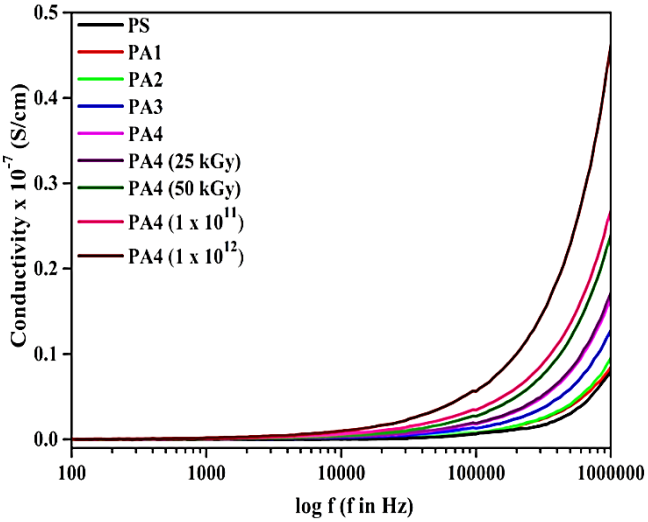

Figure 3.4 Variation in AC conductivity with frequency for polymer nanocomposites at various filler concentrations and doses.

The overall values of dielectric loss are enhanced with gamma and SHI irradiation, attributable to an increase in the number of charge carriers due to irradiation [20]. There is an exponential increase in conductivity with log frequency. The overall value of conductivity of nanocomposites increases as filler concentration and irradiation dose increase, as illustrated in **Figure 3.4**. After irradiation, the increase in the conductivity is observed due to the promotion of bonding of nanofiller to polymer and alteration of polymeric structure to hydrogen depleted carbon network. The hydrogen depleted carbon network is formed due to the extraction of hydrogen and emission of volatile gases upon irradiation [21–23].

In DSC analysis, it is observed that the glass transition temperature of polystyrene increases to a higher temperature due to the inclusion of nanoparticles. This suggests the strong interaction of polystyrene with nanoparticles and also explains the existence of constraint on the macromolecular motion [24]. After irradiation, the glass transition temperature of PA4 is observed to shift towards a lower value, which may indicate a reduction in the degree of crystallinity. Thus it is imperative to conclude that the macromolecular motion increases with the irradiation dose. After analysis of AFM image, the average surface roughness decrease due to gamma rays and ion beam irradiation. Upon SHI irradiation, polymer nanocomposites become smoother than the gamma-irradiated samples. This is due to the energy deposition by SHI irradiation higher than by gamma irradiation.

Chapter 4 discusses the effect of gamma rays and 90 MeV carbon ion beam irradiations on PS/Eu_2O_3 nanocomposites. The changes observed in structural, optical, luminescence, electrical, thermal properties, and surface morphology after gamma rays and carbon ion beam irradiations are explained in detail.

The X-ray diffraction pattern of polystyrene shows a peak centered around $2\Theta = 19.76°$, which suggests a partially crystalline nature with a dominant amorphous nature of polystyrene. The X-ray diffraction pattern of Europium (III) oxide doped polystyrene film shows typical peaks of Europium (III) oxide at $2\Theta = 16.5°$, 28.5°, 29.68°, 32.04°, 40.9° and 51.86° inscribed as (200), (222), (123), (400), (422) and (235) reflections, respectively. These comply with the BCC structure of Europium (III) oxide (JCPDS card no. 86-2476). The crystallite size of the polymeric film is seen to increase slightly with an increase in the filler concentration, whereas it slightly decreases with SHI irradiation fluence. No change in crystallite size is observed after gamma irradiation which is due to the presence of aromatic groups in polystyrene that are rarely damaged by gamma irradiation dose used [15].

FTIR transmittance spectra of synthesized polystyrene/Europium (III) oxide nanocomposites were obtained in the wavenumber range 3200-400 cm^{-1} . The intensity of peaks decreases due to the incorporation of the filler. This feature may be assigned to the interaction between polymer matrix with filler.

After gamma irradiation, there is no change in the intensity of vibrational bands of PS/Europium (III) oxide. The existence of a benzene ring in polystyrene is responsible for radiation stability [15]. In addition, The fraction of energy is used to modify the matter, while gamma rays traverse through the matter. Consequently, there is no change in the bond structure of polystyrene after gamma irradiation. But the value of LET for C^{6+} ions is too high compare to gamma rays. This large value of LET indicates that these ions are very capable of breaking off all linkage within a few nanometer areas around their trajectory

In absorption spectra of PS/Eu_2O_3 nanocomposites, two new peaks were obtained at 370 nm and 401 nm. The peaks appearing at 370 nm and 401 nm can be ascribed to $^7F_0 \rightarrow {}^5L_6$ and $^7F_0 \rightarrow {}^5D_4$ transitions of Eu^{3+} , respectively [26]. The redshift of the absorption edge has been noted with the increase in the concentration of europium (III) oxide.

It can be observed that the optical bandgap of PS/Eu_2O_3 nanocomposites decreases after gamma and SHI irradiations. The effect of gamma irradiation on optical bandgap is lower than that of SHI irradiation which may be attributed to the production of more structural disorder due to SHI irradiation. This can be explained by the density of state model in Non-crystalline solids suggested by Mott and Davis [16]. According to this model, the density of state and disorder in polymer matrices result in a decrease in bandgap and an increase in conductivity [16, 26, 27].

Photoluminescence excitation and emission spectra of pristine polymer films are shown in **Figure 4.1.** In excitation spectra, the broad peak centered at 247 nm might be ascribed to charge transfer transition between the carbonyl group of polymer matrix and Eu^{3+} ions. The emission spectra of Eu^{3+} doped polystyrene show peaks at 595 nm, 612 nm and 617 nm, which correspond to $^5D_0 \rightarrow {}^7F_1$ and $^5D_0 \rightarrow {}^7F_2$ transitions, respectively. The f-f transitions $^5D_0 \rightarrow {}^7F_1$ and $^5D_0 \rightarrow {}^7F_2$ are associated with magnetic and electric dipole transitions, respectively.

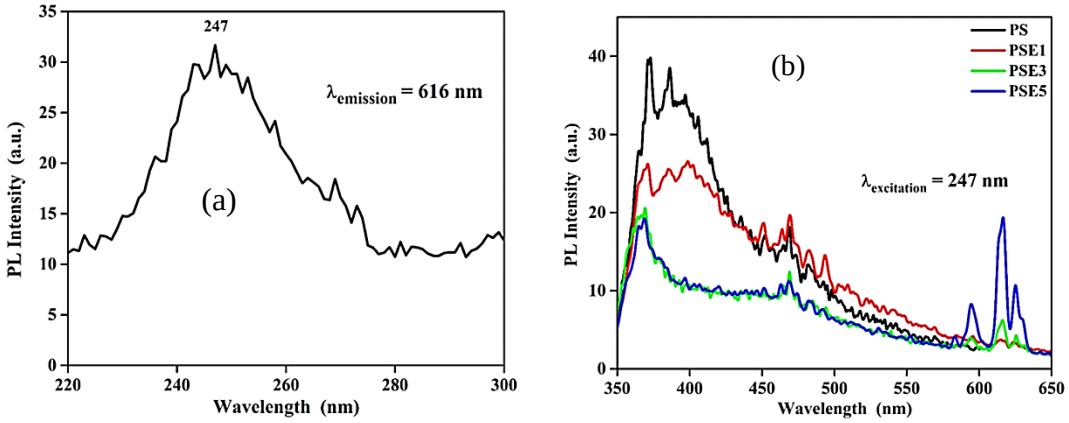

Figure 4.1 (a) Photoluminescence excitations spectrum (b) Photoluminescence emission spectra of pristine polystyrene composite films.

The intensity of characteristic peaks of Eu^{3+} ions increases with an increase in the concentration of filler. The creation of coordination bonding is associated with the augmentation of charge carriers. It serves as playing a crucial role in decreasing the activation of a singlet excitation state. It implies that the number of defects increases in polystyrene due to doping of Eu_2O_3, inferring alteration of the non-radiative and radiative recombination process. The change in the photoluminescence spectrum of PSE5 with gamma rays and SHI irradiation is shown in **Figure 4.2**. Gamma irradiation causes a decrease in the PL intensity of Eu^{3+} ions.

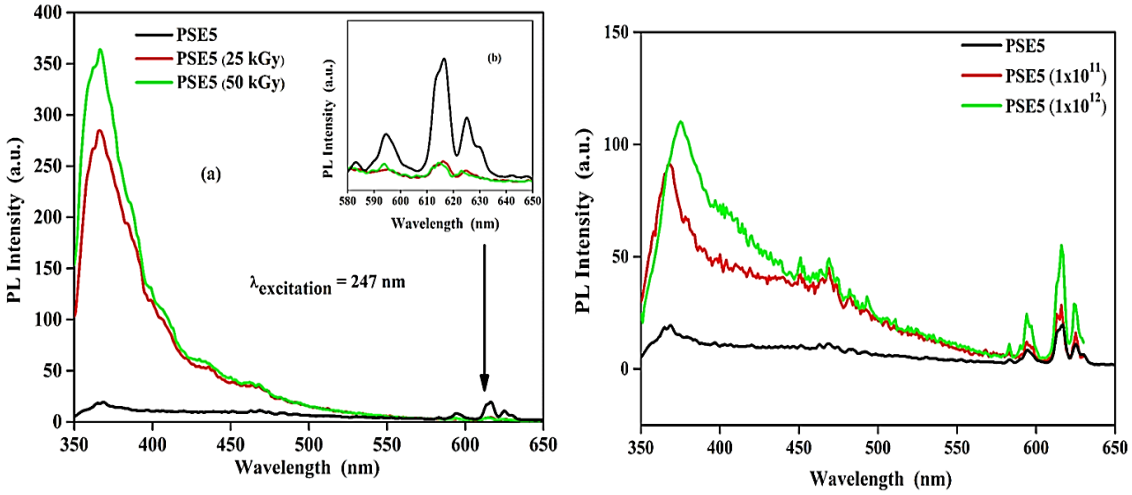

Figure 4.2 Photoluminescence emission spectra of (a) PSE5 film irradiated with gamma rays at the dose of 25 kGy and 50 kGy (b) magnified peaks in the range of 580-650 nm (c) PSE5 film irradiated with SHI irradiation**.**

In contrast, the intensity of PL emission peaks of PS and Eu^{3+} ions increases after SHI irradiation. Moreover, the irradiation may also be responsible for forming the system of conjugated bonds and carbon enriched polymer due to the extraction of hydrogen and its transformation into a graphite-like structure. The result explains the unusual behaviour of the systems after gamma irradiation.

Figures 4.3 depict TL glow curve of PS/Eu_2O_3 polymeric films irradiated with gamma rays and SHI irradiation, respectively. TL analysis of PS shows that the intensity of glow curves improves with irradiation dose. The results can be inferred to imply that the growth of trapping centers inside polymer matrix increases with irradiation dose [28].

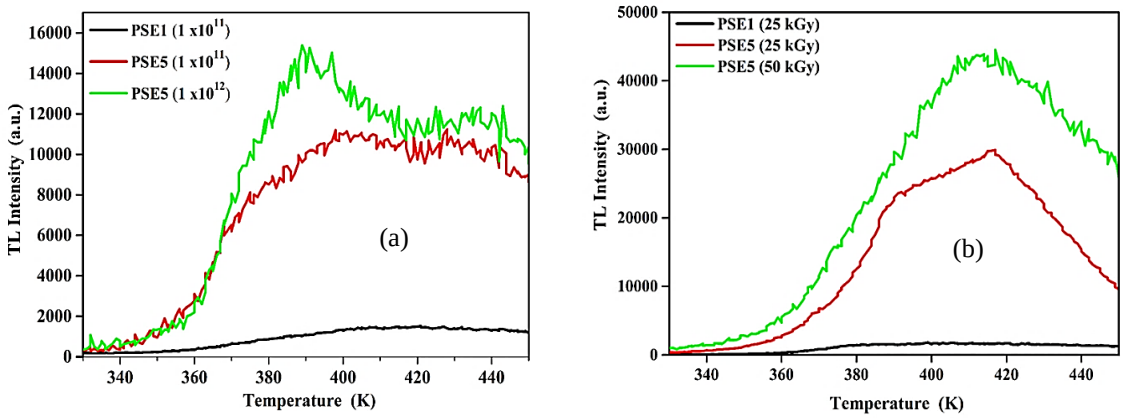

Figure 4.3 TL glow curves of (a) SHI irradiated (b) Gamma rays irradiated polymer nanocomposites.

TL analysis of PS shows that the intensity of glow curves improves with irradiation dose. The result can be inferred to imply that the growth of trapping centers inside polymer matrix increases with irradiation dose [28]. These results also correlate with the results obtained from photoluminescence analysis and suggest that PSE5 can be used for dosimetry applications [29].

The frequency-dependent dielectric constant and dielectric loss of pristine and irradiated polymeric films are depicted in **Figure 4.4**. Also, the overall value of the dielectric constant increased after irradiation which indicates that charge carriers density increases due to the scission of the polymer chain. It results in increasing interfacial polarization of space charges; as a result, the dielectric constant is observed to be increased. Due to the Swift heavy ion, Significant degradation of the sample occurs, resulted in an effective increase in the dielectric response than that of gamma irradiation.

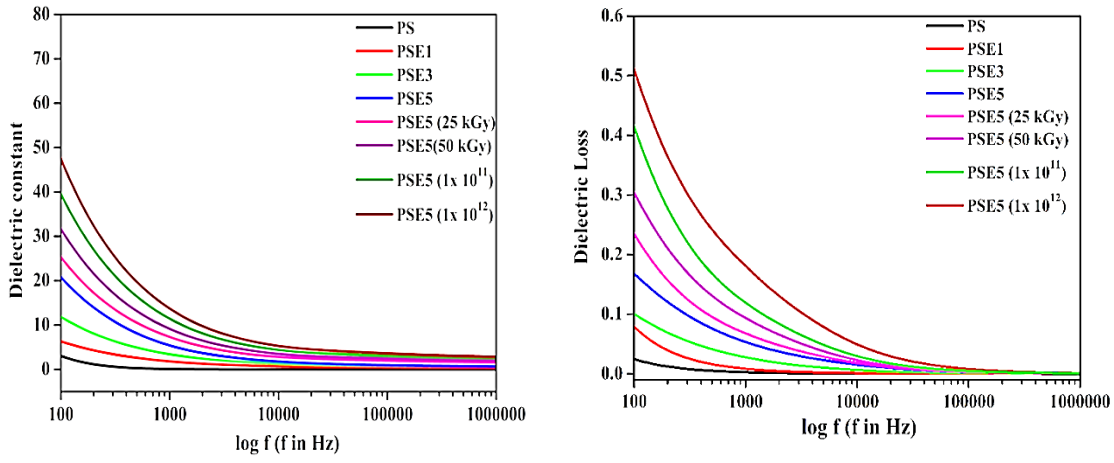

Figure 4.4 (a) Dielectric constant vs log frequency (b) Dielectric loss vs log frequency for PS/Eu_2O_3 polymer composites.

The dielectric loss increases with an increase in the concentration of filler and irradiation dose. It is due to the increase in interfacial polarization. In addition, the variation in dielectric loss of PSE5 after SHI irradiation is higher than that of gamma irradiation.

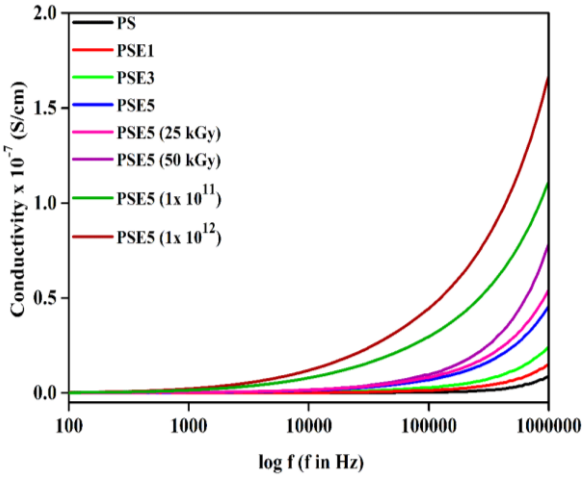

Figure 4.5 Conductivity vs log frequency for PS/Eu_2O_3 polymer composites.

Figure 4.5 illustrates AC conductivity of pristine and irradiated samples as a function of frequency, filler level and irradiation dose. It is perceived that the conductivity is increased with filler concentration. The increase in the conductivity upon the incorporation of europium (III) oxides may be attributed to the formation of several conduction paths. After irradiation, there is an increment in the AC conductivity of polymer composites with irradiation dose because of the promotion of filler to polymer bonding by irradiation. The amount of deposition of local energy increased with the gamma irradiation dose and ion fluence, indicating an increase in free electrons and impurities. In addition, the increase in A.C. conductivity of C^{6+} ion beam irradiated PSE5 is more pronounced than that of gamma-irradiated PSE5 due to the high value of LET of swift heavy ions [30].

From DSC analysis, it is observed that the Tg of the polymer matrix is displaced from 335.4 K towards higher temperature due to the incorporation of filler. The interaction of nanoparticles with polymer matrix can change the kinetics of the chain by the increase in the glass transition temperature of polystyrene [31]. After both types of irradiation, the glass transition temperature of PSE5 is observed to decrease. This fact may also suggest a decrease in the degree of crystallinity. Thus an increase of macromolecular motion with irradiation dose is imperative, and this might be caused due to the chain scission of the polymer matrix. This result is consistent with the XRD and FTIR results.

The change in surface morphology due to the incorporation of nanoparticles and irradiations was studied using Atomic Force Microscopy. The average roughness of pristine PS and PSE5 is obtained to be 9 nm and 81 nm, respectively. These results suggest that the average roughness increases due to the incorporation of filler.

Furthermore, it is suggested that polymeric films become smoother after both types of irradiations because of defect enhanced surface diffusion. Moreover, The changes in surface morphology of polymeric material due to swift heavy ion irradiation have been reported to be highly pronounced as compared to those due to gamma irradiation because swift heavy ions transfer more energy into polymer composite than gamma irradiation dose.

Chapter 5 focuses on the study of the irradiation effect on various properties of PVA/ H_3PO_4/SiO_2 nanocomposite polymer electrolytes. The structural, optical, electrical, thermal properties and surface morphology of the pristine and irradiated polymeric films have been studied using X-ray diffraction, UV-visible spectroscopy, dielectric spectroscopy, differential scanning calorimetry and AFM, respectively. The results are reported. The explanation for the influence of gamma rays and 90 MeV carbon ion beam irradiations on various properties of nanocomposite polymer electrolytes is given.

The XRD spectra of PVA/H_3PO_4/SiO_2 polymeric films indicate the semi-crystalline nature of PVA nanocomposites. X-ray diffraction (XRD) analysis of all samples revealed the change in the polymeric structure into the amorphous phase after both types of irradiation.

In FTIR spectra of pristine samples, the peaks in the region of 850-1200 cm^{-1} have been found to decrease due to the incorporation of nanoparticles. The inclusion of SiO_2 in polymer electrolytes promotes an increase in free volume. Thus, the sample becomes more amorphous [32].

After irradiation, a decreased intensity of vibration bands can be attributed to altering the bond structure due to the removal of hydrogen from the backbone and side-chain. It also suggested chain scission of the polymeric matrix. The absorption spectrum of pure PVA is characterized by an absorption band at 275 nm, which is the result of $n \rightarrow \pi^*$ transition of C=O group of polymer matrix [33]. The absorption is observed to increase with the concentration of SiO_2 nanoparticles and with irradiation dose. This could be due to the creation of a charge-transfer complex that delocalized conduction electrons. The absorption edge of PHS10 after irradiation is seen to shift towards a longer wavelength with nanofiller level and irradiation dose. The modification of indirect optical bandgap (Eg) due to the incorporation of nanoparticles and irradiation was determined using Tauc's relation [34]. The bandgap

of nanocomposite polymer electrolyte decreased due to the incorporation of nanofillers and after irradiation. The reduction in the energy bandgap due to the addition of nanoparticles highlights the interaction of polymer electrolyte with nanoparticles which is a result of the formation of localized states between HOMO and LUMO energy bands suggesting the probability of lower transition energy. Moreover, Swift heavy ions effectively produce structural disorders and more radicals in the host matrix than that of gamma irradiation which could be described based on the density of state model in amorphous solids, given by Mott and Davis [16].

The variation of the real part of complex permittivity of pristine and irradiated PHS is illustrated in **Figure 5.1.** The imaginary part of the complex permittivity of pristine and irradiated nanocomposite polymer electrolytes is shown in **Figure 5.2.** $\varepsilon'(\omega)$ and $\varepsilon''(\omega)$ are seen to increase with an increase in the concentration of SiO_2 nanoparticles which is related to the interfacial polarization effect between PVA matrix and SiO_2 nanoparticles. After irradiation, the $\varepsilon'(\omega)$ and $\varepsilon''(\omega)$ increase with an increasing dose. It could be due to enhancing the mobility of polymer chains as a result of the breaking of several bonds.

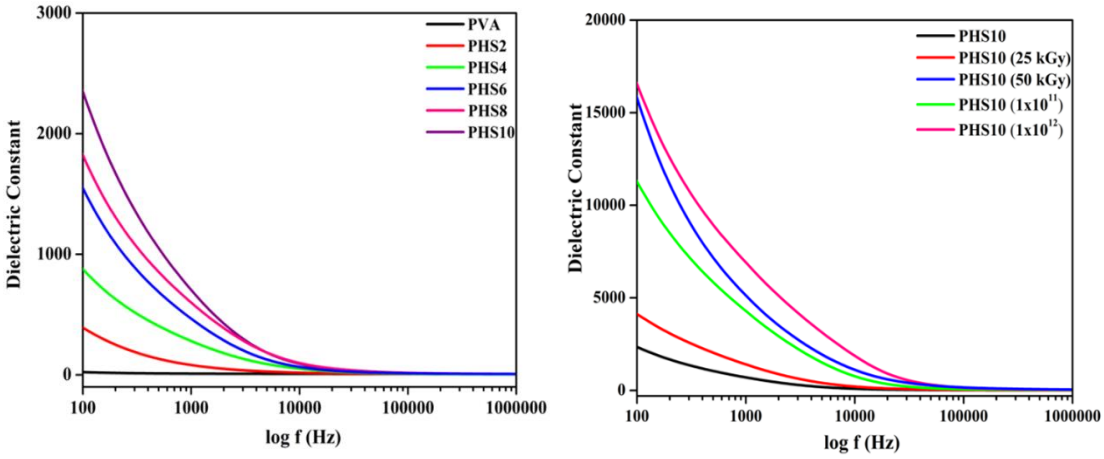

Figure 5.1 Frequency-dependent dielectric constant of PVA and, pristine and irradiated PHS nanocomposite polymer electrolytes.

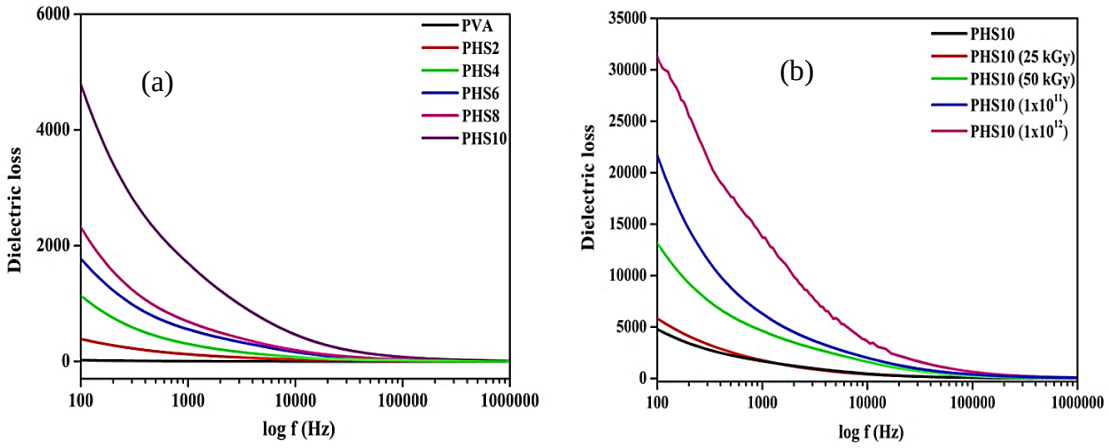

Figure 5.2 Frequency-dependent dielectric loss of (a) PVA and pristine and (b) irradiated PHS nanocomposite polymer electrolytes.

Figure 5.3 displayed a high-frequency depressed semicircle followed by a low-frequency spike. The low-frequency region is a consequence of the electrode blocking effect and the intercept of the spike on the X-axis gives the value of bulk resistance. From **Figure 5.3**, it is perceived that the value of bulk resistance decreases with increasing concentration of nanoparticles and irradiation dose. This must have enhanced amorphicity and offering a new conducting path, indicating an increase in ionic conductivity.

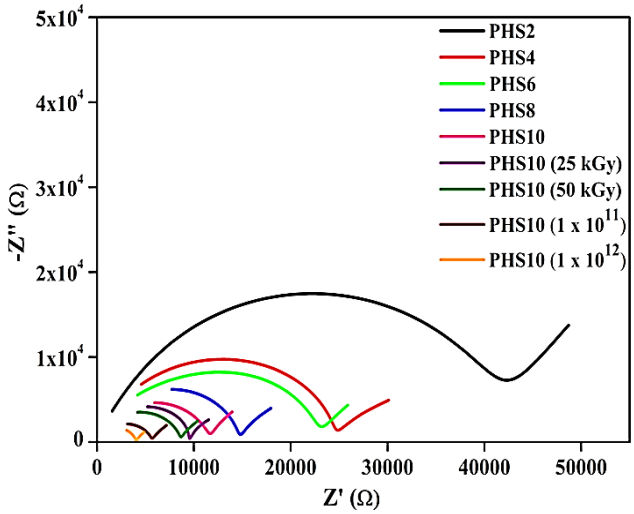

Figure 5.3 Cole-Cole plot of pristine and irradiated PHS nanocomposite polymer electrolytes.

The frequency-dependent AC conductivity plots for pristine and irradiated nanocomposite polymer electrolyte at constant temperature are shown in **Figures 5.4 & 5.5**, respectively. The increasing trend of DC conductivity can be ascribed to the reduction in crystallinity with the rising mobility of charge carriers. AC conductivity of irradiated nanocomposite polymer electrolyte is higher than that of pristine PHS.

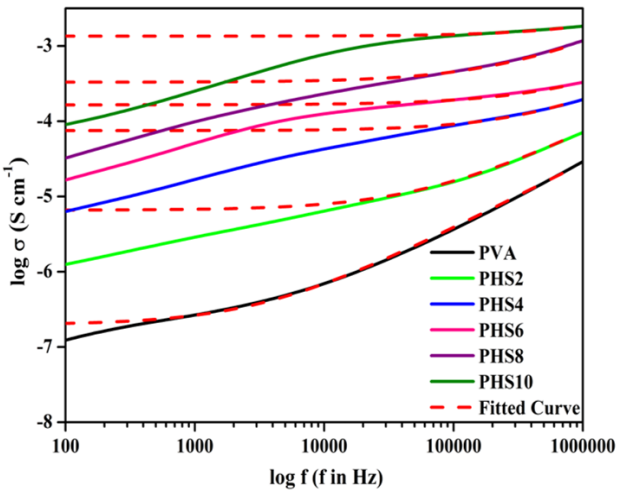

Figure 5.4 Frequency-dependent AC conductivity of PVA and pristine PHS nanocomposite polymer electrolytes.

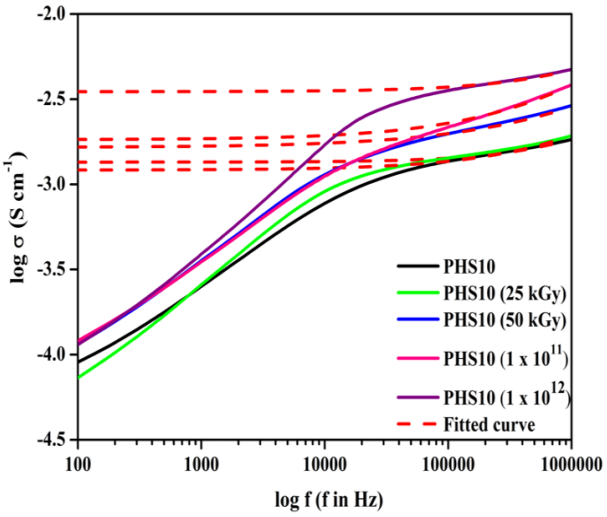

Figure 5.5 Frequency-dependent AC conductivity of PVA and irradiated PHS10 nanocomposite polymer electrolytes.

The effect of irradiation on the thermal properties and degree of crystallinity of PHS10 were investigated using DSC thermograms. The relative change in the value of the degree of crystallinity (ΔX%) of PHS10 is reduced due to gamma and SHI irradiation, respectively. The melting point of PHS10 is observed to shift towards the lower temperature after irradiation, suggesting a decrease of molecular weight due to the scission of the polymer chain.

Three-dimensional scanned topographical image of pristine and irradiated nanocomposite polymer electrolytes was obtained using AFM in tapping mode. It was analyzed by means of average surface roughness (Ra). The obtained average roughness Ra of pristine PHS10 was found to be 92 nm, that of SHI irradiated

PHS10(1 x $10^{12}_{ions/cm2}$) and gamma-irradiated PHS10 (50kGy) is 82 nm and 86 nm, respectively. The roughness changes detected in the case of gamma irradiation are less than those in the case of ion beam irradiation due to the lesser transfer of energy by gamma radiation than by ions [1]**.** Thus the surface of irradiated polymeric material became smoother than the pristine polymeric material. The decrease in surface roughness indicates increasing the ionic conductivity of the material.

Chapter 6 This chapter summarizes the work carried out and highlights its significant conclusions together with the future scope of work.

.

References:

[1] B. S. Rathore, M. S. Gaur, K. S. Singh, Investigation of thermally stimulated properties of SHI beam irradiated polycarbonate/polystyrene double layered samples, Nucl. Instruments Methods Phys. Res. Sect. B Beam Interact. with Mater. Atoms. 269 (2011) 2792–2797. https://doi.org/10.1016/j.nimb.2011.09.003.

[2] P. Maji, R. B. Choudhary, M. Majhi, Structural, optical and dielectric properties of ZrO2 reinforced polymeric nanocomposite films of polymethylmethacrylate (PMMA), Optik 127 (2016) 4848–4853.

[3] M. R. Becker, V. Stefani, R. R. B. Correia, C. Bubeck, M. Jahja, M. M. C. Forte, Waveguide optical properties of polystyrene doped with p-nitroaniline derivatives, Opt. Mater. 32 (2010) 1526–1531. https://doi.org/10.1016/j.optmat.2010.06.015.

[4] B. A. Rozenberg, R. Tenne, Polymer-assisted fabrication of nanoparticles and 8https://doi.org/10.1016/j.progpolymsci.2007.07.004.

[5] A. P. Indolia, M. S. Gaur, Optical properties of solution grown PVDF-ZnO nanocomposite thin films, J. Polym. Res. 20 (2013) 43. https://doi.org/10.1007/s10965-012-0043-y.

[6] P. L. Forster, D. F. Parra, J. Kai, H. F. Brito, A. B. Lugao, Influence of gamma irradiation on photoluminescence properties of polycarbonate films doped with Eu^{3+}-B-diketonate complex, Radiat. Phys. Chem. 84 (2013) 47–50. https://doi.org/10.1016/j.radphyschem.2012.06.046.

[7] R. J. Sengwa, S. Choudhary, Dielectric and electrical properties of PEO– Al_2O_3 nanocomposites, J. Alloys Compd. 701 (2017) 652–659. https://doi.org/10.1016/j.jallcom.2017.01.155.

[8] S. Ningaraju, A. P. Gnana Prakash, H. B. Ravikumar, Studies on free volume controlled electrical properties of PVA/NiO and PVA/TiO_2 polymer nanocomposites, Solid State Ionics. 320 (2018) 132–147. https://doi.org/10.1016/j.ssi.2018.03.006.

[9] I. Ali, G. A. Meligi, M. R. Akl, T. A. Saleh, Influence of γ-ray irradiation doses on physicochemical properties of silver polystyrene polyvinyl pyrrolidone nanocomposites, Mater. Chem. Phys. 226 (2019) 250–256. https://doi.org/10.1016/j.matchemphys.2018.12.084.

[10] S. Asad Ali, R. Kumar, P. M. G. Nambissan, F. Singh, R. Prasad, Positron annihilation lifetime and Doppler broadening study in 50 MeV Li^{3+} ion irradiated polystyrene 28 films, Nucl. Instruments Methods Phys. Res. Sect. B Beam Interact. with Mater. Atoms. 268 (2010) 1809–1812. https://doi.org/10.1016/j.nimb.2010.02.080.

[11] H. Tahara, T. Kawabata, L. Zhang, T. Yasui, T. Yoshikawa, Exposure of spacecraft polymers to energetic ions, electrons and ultraviolet light, Nucl. Instruments Methods Phys. Res. Sect. B Beam Interact. with Mater. Atoms. 121 (1997) 446–449. https://doi.org/10.1016/S0168-583X(96)00600-3.

[12] A. Qureshi, N. L. Singh, S. Shah, P. Kulriya, F. Singh, D. K. Avasthi, Modification of polymer composite films using 120 MeV Ni^{10+} ions, Nucl. Instruments Methods Phys. Res. Sect. B Beam Interact. with Mater. Atoms. 266 (2008) 1775–1779. https://doi.org/10.1016/j.nimb.2008.01.057.

[13] R. Singhal, A. Kumar, Y. K. Mishra, S. Mohapatra, J. C. Pivin, D. K. Avasthi, Swift heavy ion induced modifications of fullerene C70 thin films, Nucl. Instruments Methods Phys. Res. Sect. B Beam Interact. with Mater. Atoms. 266 (2008) 3257–3262. https://doi.org/10.1016/j.nimb.2008.04.003.

[14] S. Kumar, P. Singh, R.G. Sonkawade, K. Awasthi, R. Kumar, 60 MeV Ni ion induced modifications in nano-CdS / polystyrene composite films, 94 (2014) 49–53.

[15] R. Mishra, S. P. Tripathy, D. Sinha, K. K. Dwivedi, S. Ghosh, D. T. Khathing, M. Müller, D. Fink, W. H. Chung, Optical and electrical properties of some electron and proton irradiated polymers, Nucl. Inst. Meth. Phys. Res. Sect. B Beam Interact. with Mater. Atoms. 168 (2000) 59–64. https://doi.org/10.1016/S0168-583X(99)00829-0.

[16] N. F. Mott, E.A. Davis, Electronic Processes in Non Crystalline Materials, Clarendon Press, Oxford, 1979.

[17] S. Tóth, M. Füle, M. Veres, I. Pócsik, M. Koós, A. Tóth, T. Ujvári, I. Bertóti, Photoluminescence of ultra-high molecular weight polyethylene modified by fast atom bombardment, Thin Solid Films. 497 (2006) 279–283. https://doi.org/10.1016/j.tsf.2005.10.050.

[18] G. B. Hadjichristov, I. L. Stefanov, B. I. Florian, G. D. Blaskova, V. G. Ivanov, E. Faulques, Optical reflectivity study of silicon ion implanted poly (methyl methacrylate), Appl. Surf. Sci. 256 (2009) 779–786. https://doi.org/10.1016/j.apsusc.2009.08.059.

[19] N. J. Shivaramu, B. N. Lakshminarasappa, F. Singh, E. Coetsee, H. C. Swart, Thermoluminescence response in ^{60}Co gamma rays, 100 MeV Si^{8+} and 150 MeV Au^{9+} irradiated Y_2O_3:Ho^{3+} nanophosphor, J. Alloys Compd. 778 (2019) 554–565. https://doi.org/10.1016/j.jallcom.2018.11.185.

[20] T. Phukan, D. Kanjilal, T. D. Goswami, H. L. Das, Dielectric response of irradiated PADC polymer track detector, Nucl. Instruments Methods Phys. Res. Sect. B Beam Interact. with Mater. Atoms. 234 (2005) 520–524. https://doi.org/10.1016/j.nimb.2005.02.022.

[21] A. Qureshi, D. Singh, N. L. Singh, S. Ataoglu, A. N. Gulluoglu, A. Tripathi, D. K. Avasthi, Effect of irradiation by 140 Mev Ag^{11+} ions on the optical and electrical properties of polypropylene/TiO_2 composite, Nucl. Inst. Meth. Phys. Res. 30 Sect. B Beam Interact. with Mater. Atoms. 267 (2009) 3456–3460. https://doi.org/10.1016/j.nimb.2009.07.016.

[22] N. L. Singh, A. Sharma, D. K. Avasthi, V. Shrinet, Temperature and frequency dependent electrical properties of 50 MeV Li^{3+} ion irradiated polymeric blends, Radiat. Eff. Def. Sol. 160 (2005) 99–107. https://doi.org/10.1080/10420150500116649.

[23] D. Fink, W. H. Chung, R. Klett, A. Schmoldt, J. Cardoso, R. Montiel, M.H. Vazquez, L. Wang, F. Hosoi, H. Omichi, P. Goppelt-Langer, Carbonaceous clusters in irradiated polymers as revealed by UV-Vis spectrometry, Radiat. Eff. Def. Sol. 133 (1995) 193–208. https://doi.org/10.1080/10420159508223990.

[24] S. Ningaraju, H.B. Ravikumar, Ionic and electronic transport in PSF/NiO and PSF/TiO_2 polymer nanocomposites: A positron lifetime study, Solid State Ionics. 310 (2017) 81–94. https://doi.org/10.1016/j.ssi.2017.08.009.

[25] S. Rada, A. Dehelean, E. Culea, FTIR and UV–VIS spectroscopy investigations on the structure of the europium–lead–tellurate glasses, J. Non. Cryst. Solids. 357 (2011) 3070–3073. https://doi.org/10.1016/j.jnoncrysol.2011.04.013.

[26] A. A. El-Saftawy, A. M. Abdel Reheem, S. A. Kandil, S. A. Abd El Aal, S. Salama, Comparative studies on PADC polymeric detector treated by gamma radiation and Ar ion beam, Appl. Surf. Sci. 371 (2016) 596–606. https://doi.org/10.1016/j.apsusc.2016.03.044.

[27] R. K. Dhillon, P. Singh, S. K. Gupta, S. Singh, R. Kumar, Study of high energy (MeV) N^{6+} ion and gamma radiation induced modifications in low density polyethylene (LDPE) polymer, Nucl. Instruments Methods Phys. Res. Sect. B Beam Interact. with Mater. Atoms. 301 (2013) 12–16. https://doi.org/10.1016/j.nimb.2013.02.014.

[28] S. Som, A. Choubey, S. K. Sharma, Luminescence studies of rare earth doped yttrium gadolinium mixed oxide phosphor, 407 (2012) 3515–3519.

[29] N. A. Kazakis, N.C. Tsirliganis, G. Kitis, Preliminary thermoluminescence investigation of commercial pharmaceutical glass containers towards the sterilization dosimetry of liquid drugs, Appl. Radiat. Isot. 105 (2015) 130–138. https://doi.org/10.1016/j.apradiso.2015.08.005.

[30] E. Lee, G. Rao, L. Mansur, LET effect on cross-linking and scission mechanisms of PMMA during irradiation, Radiat. Phys. Chem. 55 (1999) 293–305. https://doi.org/10.1016/S0969-806X(99)00184-X.

[31] V. V. Vodnik, D. K. Božanić, E. Džunuzović, J. Vuković, J. M. Nedeljković, Thermal and optical properties of silver–poly(methylmethacrylate) nanocomposites prepared by in-situ radical polymerization, Eur. Polym. J. 46 (2010) 137–144. https://doi.org/10.1016/j.eurpolymj.2009.10.022.

[32] J. Jiang, D. Gao, Z. Li, G. Su, Gel polymer electrolytes prepared by in situ polymerization of vinyl monomers in room-temperature ionic liquids, React. Funct. Polym. 66 (2006) 1141–1148. https://doi.org/10.1016/j.reactfunctpolym.2006.02.004.

[33] R. P. Chahal, S. Mahendia, A. K. Tomar, S. Kumar, γ-Irradiated PVA/Ag nanocomposite films: Materials for optical applications, J. Alloys Compd. 538 (2012) 212–219. https://doi.org/10.1016/j.jallcom.2012.05.085.

[34] J. Tauc, R. Grigorovici, A. Vancu, Optical Properties and Electronic Structure of Amorphous Germanium, Phys. Status Solidi. 15 (1966) 627–637. https://doi.org/10.1002/pssb.19660150224